ARTICLE IN PRESS
BBABIO-47348; No. of pages: 12; 4C: 2, 4, 6, 7, 8, 9
Biochimica et Biophysica Acta xxx (2014) xxx–xxx
Contents lists available at ScienceDirect
Biochimica et Biophysica Acta
journal homepage: www.elsevier.com/locate/bbabio

High yield of secondary B-side electron transfer in mutant *Rhodobacter capsulatus* reaction centers

Lucas Kressel [a,1], Kaitlyn Faries [b,1], Marc J. Wander [a], Charles E. Zogzas [a], Rachel J. Mejdrich [a], Deborah K. Hanson [a], Dewey Holten [b], Philip D. Laible [a], Christine Kirmaier [b]

[a] Biosciences Division, Argonne National Laboratory, Argonne, IL 60439, USA
[b] Department of Chemistry, Washington University, St. Louis, MO 63130, USA

ARTICLE INFO

Article history:
Received 10 June 2014
Received in revised form 22 July 2014
Accepted 26 July 2014
Available online xxxx

Keywords:
Photosynthetic reaction center
Charge recombination
High-throughput screening
Ultrafast spectroscopy
Directed evolution
Transmembrane electron transfer

ABSTRACT

From the crystal structures of reaction centers (RCs) from purple photosynthetic bacteria, two pathways for electron transfer (ET) are apparent but only one pathway (the A side) operates in the native protein-cofactor complex. Partial activation of the B-side pathway has unveiled the true inefficiencies of ET processes on that side in comparison to analogous reactions on the A side. Of significance are the relative rate constants for forward ET and the competing charge recombination reactions. On the B side, these rate constants are nearly equal for the secondary charge-separation step (ET from bacteriopheophytin to quinone), relegating the yield of this process to <50%. Herein we report efforts to optimize this step. In surveying all possible residues at position 131 in the M subunit, we discovered that when glutamic acid replaces the native valine the efficiency of the secondary ET is nearly two-fold higher than in the wild-type RC. The positive effect of M131 Glu is likely due to formation of a hydrogen bond with the ring-V keto group of the B-side bacteriopheophytin leading to stabilization of the charge-separated state involving this cofactor. This change slows charge recombination by roughly a factor of two and affords the improved yield of the desired forward ET to the B-side quinone terminal acceptor.

1. Introduction

The bacterial photosynthetic reaction center (RC) is a transmembrane protein–cofactor complex that converts light energy into chemical potential for use in cellular processes. Of the three protein subunits (L, M and H), homologous L and M comprise an integral core and bind a bacteriochlorophyll (BChl) dimer (P) that is the primary electron donor, two monomeric BChls (B), two monomeric bacteriopheophytins (H) and two quinones (Q). These cofactors are arranged in two branches (A and B) in pseudo-C_2 symmetry (Fig. 1A) [1–4]. Despite the similarity between the branches, in the wild-type (WT) RC only the A-side cofactors participate in rapid multi-step electron transfer (ET) that results in nearly quantitative formation of $P^+Q_A^-$ from P^* in less than a nanosecond. Subsequent $P^+Q_A^- \rightarrow P^+Q_B^-$ ET occurs on the microsecond timescale.

Site-directed mutagenesis has been used with great success over the last 25 years to explore the factors responsible for unidirectional A-side ET in the RC. Mutant RCs that perform B-side charge separation – albeit generally in low yield – have enriched our understanding of the mechanism of primary A-side charge separation and framed views of how ET from P^* to the B-side cofactors is normally suppressed [5–25]. The general working model (Fig. 1B) is that the $P^+B_A^-$ state is positioned between P^* and $P^+H_A^-$ supporting two initial ET steps, $P^* \rightarrow P^+B_A^- \rightarrow P^+H_A^-$, that occur on the ~0.5 to ~5 ps timescale [26–36]. On the B side, $P^* \rightarrow P^+H_B^-$ ET is much slower (~100–200 ps) with $P^+B_B^-$ thought to be higher in free energy than P^* and supporting ET by a superexchange mechanism. Distinctions also exist between the intrinsic properties of $P^+H_A^-$ and $P^+H_B^-$. $P^+H_A^- \rightarrow P^+Q_A^-$ ET occurs in 200 ps. In the absence of ET, $P^+H_A^-$ lives for 10–20 ns and decays by charge recombination (CR) to form the ground and triplet excited states [28,34]. In comparison, $P^+H_B^- \rightarrow P^+Q_B^-$ ET is much slower (~4 ns time constant) and $P^+H_B^-$ has a shorter intrinsic lifetime (~3 ns) [23]. This combination results in ~45% yield of $P^+H_B^- \rightarrow P^+Q_B^-$ ET compared to 100% formation of $P^+Q_A^-$ on the A side. Therefore, even if a high yield of P^* conversion to $P^+H_B^-$ is achieved in a mutant, translation of that increase through to a high yield of $P^+Q_B^-$ is not assured. To achieve this end, the mutant RC would also require changes that increase the rate constant for $P^+H_B^- \rightarrow P^+Q_B^-$ ET and/or reduce the rate constant for $P^+H_B^-$ CR.

We have adopted a directed molecular evolution approach to engineering the RC to enable efficient B-branch ET that employs *Rhodobacter* (*Rb.*) *capsulatus* and rapid, efficient, semi-random methods for constructing RC mutants. This is coupled to a high-throughput millisecond screening assay (ms assay) that measures the yield of $P^+Q_B^-$ formed solely via the B-branch cofactors [37]. In this work we report on two groups of mutant RCs, seeking mutations that increase the rate of $P^+H_B^- \rightarrow P^+Q_B^-$ ET and/or decrease the rates of the competing CR processes of $P^+H_B^-$. The first mutant set targets residue M131 near H_B (Fig. 1A), where a Val is the native amino acid in *Rb. capsulatus* (Thr in *Rb. sphaeroides*). All amino acids were substituted at M131 ("saturation mutagenesis"), mutants denoted V(M131)X. The motivation for

http://dx.doi.org/10.1016/j.bbabio.2014.07.015
0005-2728/© 2014 Published by Elsevier B.V.

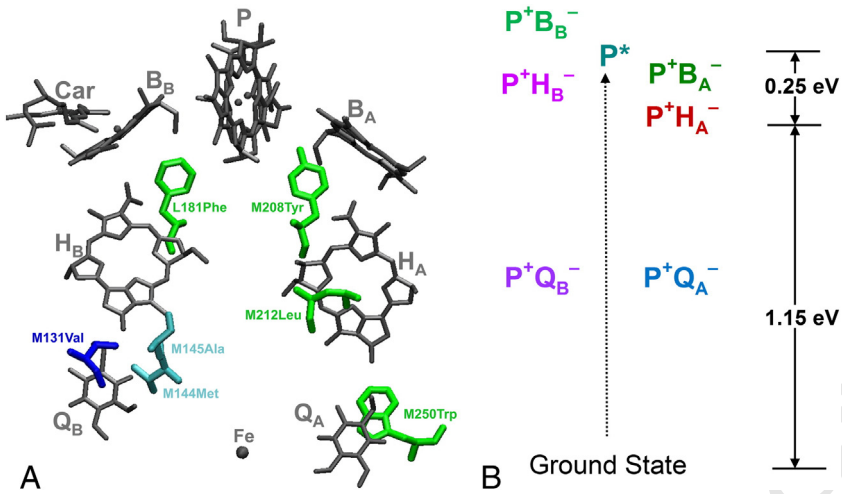

Fig. 1. (A) Positions of the substituted amino acids relative to the cofactors in the RC, from the *Rb. sphaeroides* crystal structure 1PCR [4]. Native amino acids are shown. Sites that comprise the YFHV background mutations are in green. The M131 site that was subject to extensive mutation here is in blue. The M144 and M145 sites also studied here are in cyan. See Table 1 for additional details. (B) Model free energy diagram for WT RCs.

exploring M131 is that the C_2 symmetry-related residue on the A side is a Glu (at L104) that forms a hydrogen bond with H_A [1] and previous work has suggested that an Asp at M131 (or at M133 in *Rb. sphaeroides*) forms a hydrogen bond to H_B. [10,25,38,39] The second group couples substitution of all 20 amino acids at M131 with mutations of M144Met to Ile and M145Ala to Ser (designated "IS"). Residues M144–145 are located somewhat between H_B and Q_B (Fig. 1A) and the IS substitutions were identified by Youvan and coworkers in a photocompetent phenotypic revertant of a strain carrying multiple-site mutations in the Q_B binding pocket [40,41].

We find an increased yield of $P^+Q_B^-$ from B-side ET in RCs carrying amino acid substitutions at M131, for the IS pair alone, and for some substitutions at M131 paired with the IS mutations. Of these, five mutants were selected for further investigation of ET to and between the B-side cofactors using ultrafast transient absorption (TA) spectroscopy in order to determine the origin of improved $P^+Q_B^-$ production. Among the selected mutants, we find that the yields of initial $P^* \rightarrow P^+H_B^-$ ET are essentially identical and the relative higher/lower yields of $P^+Q_B^-$ derive from a rebalancing of the rate constants for the competing $P^+H_B^- \rightarrow P^+Q_B^-$ ET and $P^+H_B^-$ CR processes.

2. Material and methods

2.1. Preparation of mutants and RCs

The V(M131)X and V(M131)X+IS mutations were created in derivatives of a specifically engineered expression plasmid, pBBRKW2HTsLsM [37]. This plasmid contains strategically-placed unique restriction enzyme sites in the L and M genes that enable rapid cassette-based mutagenesis of regions near the RC cofactors. Each V(M131)X mutation was carried on a cassette flanked by *Eco*RV and *Xma*I restriction enzyme sites and the M(M144)I-A(M145)S mutations were carried on a fragment bearing *Xma*I and *Afl*II ends. In a small subset of mutant plasmids, a synthetic cassette encoding the native Trp residue at M250 was used to replace a region flanked by unique *Nhe*I and *Nco*I sites. All mutations were verified by sequencing of candidate plasmids. RCs were expressed in *Rb. capsulatus* host strain U43 following conjugal transfer of mutant plasmids. RC expression screening and RC purification followed methods described previously [37]. Purified RCs were suspended in 10 mM Tris (pH 7.8), 0.1% Deriphat 160-C for all spectroscopic experiments.

2.2. Millisecond screening assay

The $P^+Q_B^-$ yield in the mutant RCs was determined using a dedicated apparatus of local design that allows studies spanning ~100 μs to ~5 min. [37] Samples, ~100 μl in volume and having $A_{865nm} = 0.05 \pm 0.005$ in a 2 mm pathlength, were arrayed and screened in 96-well plates. RCs were excited with a single ~7 ns excitation flash at 532 nm (provided by a Q-switched Nd:YAG laser) and the magnitude and decay of bleaching of the ground state absorbance of P were probed at 850 nm (provided by a continuous-wave diode laser). As controls, RCs from WT and the YFHV mutant (defined in Section 3.1) were included on every screening plate. The WT RC provides the reference of ~100% $P^+Q_B^-$ formation (from $P^+Q_A^-$) and the YFHV RC gives ~22% yield of $P^+Q_B^-$ formation via B-side ET.

2.3. Ultrafast transient absorption (TA) spectroscopy

Ultrafast TA experiments employed ~130 fs excitation and white light probe flashes at 10 Hz and an apparatus described previously [8]. Data were acquired in an ~220-nm spectral window. For experiments that probed 480–700 nm, RCs had A_{865nm} = ~0.9–1.0 (2 mm pathlength). Experiments probing 830–1050 nm utilized RCs with A_{865nm} = ~0.5–0.6 (2 mm pathlength). To ensure that fresh sample was excited on each laser flash, 2.0–2.5 ml of RCs were flowed rapidly through a 2 mm path-length cell and an ice-cooled (~10 °C) reservoir.

2.4. Extended-timescale ultrafast TA measurements

TA measurements on the ~0.5 ns to 450 μs timescale utilized 1 KHz, ~130-fs excitation flashes at 865 nm provided by an amplified (Spitfire Ace) Ti:sapphire (MaiTai) laser system (Spectra Physics) coupled to a Topaz (Light Conversion) optical parametric amplifier. An EOS detection system (Ultrafast Systems Inc.) provided ~1 ns white light probe light flashes that are slaved to the 1 kHz clock of the ultrafast laser system. The instrument response function (if viewed as a Gaussian) of the EOS detection system is ~0.5 ns. TA spectra (400–800 nm window) were averaged into "bins" (100 ps minimum width) with 450 μs being the longest delay time possible at a 1 kHz repetition rate. RC samples used for these experiments were stirred rapidly and contained terbutryn (tb), a competitive inhibitor of Q_B binding. In particular, 10–13 μL of a

Please cite this article as: L. Kressel, et al., High yield of secondary B-side electron transfer in mutant Rhodobacter capsulatus reaction centers, Biochim. Biophys. Acta (2014), http://dx.doi.org/10.1016/j.bbabio.2014.07.015